IEEE Access
Multidisciplinary | Rapid Review | Open Access Journal

Received 30 July 2022, accepted 19 August 2022, date of publication 23 August 2022, date of current version 29 August 2022.

Digital Object Identifier 10.1109/ACCESS.2022.3201020

RESEARCH ARTICLE

Numerical Investigation of Photonic Crystal Fiber-Based Biosensor for Pathogens Detection in Water

EMRANUL HAQUE, ABDULLAH AL NOMAN, (Member, IEEE), AND FEROZ AHMED, (Member, IEEE)
Department of Electrical and Electronic Engineering, Independent University, Bangladesh, Dhaka 1229, Bangladesh
Corresponding author: Emranul Haque (emran1612@iub.edu.bd)

This work was supported by Independent University, Bangladesh.

ABSTRACT In this paper, a Photonic Crystal Fiber (PCF) based Surface Plasmon Resonance (SPR) biosensor for the detection of four bacteria such as *Vibrio Cholera, Escherichia Coli (E. coli), Bacillus Anthracis, and Enterococcus Faecalis* is proposed and evaluated numerically using finite element method (FEM)-based simulation tool. The proposed sensor exhibits excellent performance characteristics and has the configuration of identifying analyte samples externally. The sensor is designed with a basic square lattice of PCF, covered with a thin chemically stable gold layer. The proposed sensor can detect these four bacteria from pure water and has the highest wavelength sensitivity of 5161 nm/RIU for *Enterococcus Faecalis.* Other critical parameters such as Signal to Noise Ratio, Detection Limit, Sensor Length, Quality Factor, and Detection Accuracy are also calculated and presented for the proposed PCF biosensor.

INDEX TERMS PCF, bacteria detection, biosensor, refractive index.

I. INTRODUCTION

Bacteria can be found almost anywhere, including on the surface and beneath waterways. Some of these microorganisms have the potential to be harmful to human health. Many outbreaks have been linked to waterborne diseases caused by a variety of bacteria, viruses, and protozoa such as diarrhea and other gastrointestinal illnesses [1].

Contamination of water resources by water-borne pathogens and the diseases they cause are serious concerns for water quality around the world [1]. *E. Coli, Vibrio Cholera,* and *Salmonella Typhi* are the three most common pathogens that cause water pollution. Symptoms such as nausea, vomiting, stomach pain, diarrhea, and cramping are brought on by the presence of these pathogenic organisms. Infected by *E. coli* O157: H17 pathogenic in drinking water caused the deaths of seven people and more than 2300 illnesses in Ontario, Canada in the year 2000 [2].

Studies have shown methodologies of diagnosing bacteria that include pathogen binding mechanisms and antigen capture tactics, such as antigen–antibody and aptamer–ligand interactions [3], [4]. Techniques such as gene sequencing, polymerase chain reaction (PCR), fluorescence methods, mass spectrometry, and enzyme-linked immunosorbent assays (ELISA) are used in current diagnostic processes [5], [6], [7], [8], [9], [10], [11], [12]. While all these bioanalytical techniques are quite precise, they each have their own set of drawbacks. It is important to note that the fluorescence method requires labeling samples with a fluorescent probe; mass spectrometry analysis of several samples is time-consuming; and all these techniques are generally expensive with high response times, as well as require specialized equipment [13]. It has recently emerged that bioanalytical approaches using optical biosensors can overcome these constraints. [14].

Next-generation technologies such as plasmonic-based sensing, which allow biosensors to be reduced in size while increasing detection throughput and decreasing operating costs are currently being developed [15]. Surface Plasmon Resonance (SPR), localized SPR, surface-enhanced Raman scattering, surface-enhanced infrared absorption spectroscopy, and surface-enhanced fluorescence can all be

The associate editor coordinating the review of this manuscript and approving it for publication was Norbert Herencsar.

used to detect pathogens [16]. A promising new way to identify pathogens rapidly and with great sensitivity, SPR-based sensing techniques are among these revolutionary ways, and this technology has started to displace other conventional diagnostic approaches [17]. Varsha Sharma *et al.* developed a photonic crystal-based four-channel nano-cavity ring resonator to detect Vibrio Cholera and E. Coli bacterium of single molecule in pure drinking water with quality factor of 344 and 309, respectively [18].

SPR arises at the interface between two materials with opposing permittivity because of a transverse magnetically (TM) polarized light that stimulates the oscillation of conduction electrons. Photon energy is consumed by the oscillating free electrons at the contact, resulting in the formation and propagation of surface plasmon waves (SPWs). In the case of biological samples that are sensitive to an electromagnetic field, sample SPR peak deflection is a possible drawback of SPR sensors [19]. However, these disadvantages are more than offset by four key benefits: Non-destructive and non-invasive means that the sample is not damaged or physiochemically transformed in any way; sensitive optical quantification of the interaction between molecules in real-time without the need for a separate probe using a radioactive or fluorescent material; and reactivation of the sensor surface after detection of the target analyte for up to three additional times [20], [21], [22], [23], [24]. Aside from these advantages, this method is fast, accurate, and cost-effective; it does not require specialist training, and it can be applied to a wide range of targets [25], [26], [27].

Gold (Au) and silver (Ag) are two of the most often utilized plasmonic materials in SPR sensors, which have a significant impact on their performance. However, Au is resistant to oxidation and erosion in a variety of conditions makes it the chosen metal. Au also has a higher wavelength shift, making it easier to precisely detect an unknown analyte [28]. When compared to gold, silver has a distinct resonance peak, although it oxidizes quite quickly [29]. As a result, gold is frequently employed as a plasmonic material because of its better chemical stability and performance [30].

In this paper, the detection of four bacteria like *Vibrio Cholera, E. Coli, Bacillus Anthracis,* and *Enterococcus Faecalis* is studied for their presence in the drinking water. All these bacteria are potent to cause major damage to human health. For the detection purpose, a PCF-SPR biosensor has been proposed. Plasmonic material gold is chosen and coated over the d-shaped surface of the sensor. Simulation results show that the proposed sensor can detect these bacteria with the highest sensitivity of 5161 nm/RIU for single molecule *Enterococcus Faecalis*.

II. PCF BIOSENSOR STRUCTURE

The schematic diagram of the proposed PCF biosensor for the detection of bacteria is illustrated in Fig. 1 (a). A Square lattice-D-shaped structure with a single layer of circular air holes fills the background of the silica substance. The diameter of the air holes (d_1) is 1.5 μm. The pitch ($\wedge$) value of the square lattice structure is 3.3 μm. The ''stacking and drawing'' method is the most common fabrication method for the proposed PCF [31]. Gold (Au) is coated on the PCF's d-shaped surface as an exterior layer. The thickness of the Au or plasmonic layer is 200 nm. The values of the air hole diameter, pitch, and thickness of plasmonic material stated are the optimized values for the proposed sensor structure. Several material coatings processes such as ''Wet chemical deposition'', ''Radio frequency sputtering (RF sputtering)'', and even ''thermal evaporation'' can be used to deposit this exterior thin layer [32]. To get a consistent layer thickness, several common ways of metal coating are put to the test. When it comes to nanometer-thick metal coatings, ''chemical vapor deposition (CVD)'' is an effective method [32]. A biochemical layer that is loaded with analyte samples to detect bacteria is placed at the outside circumference of the fiber structure. The ''selective-filling approach'' demonstrated in theoretical and experimental research can be utilized to fill the analyte sample into the biochemical layer [33]. The scattering boundary conditions have been applied to a circular perfectly matched layer (PML) layer to absorb radiation energy from the PCF's surface. Using Sellmeier's equation no. 1, the refractive index (RI) of the background material is calculated [34].

$$n^2_{sio_2}(\lambda) = 1 + \frac{B_1\lambda^2}{\lambda^2 - C_1} + \frac{B_2\lambda^2}{\lambda^2 - C_2} + \frac{B_3\lambda^2}{\lambda^2 - C_3} \quad (1)$$

where, B_1, B_2, B_3, C_1, C_2, and C_3 are the Sellmeier coefficients, n is the RI for pure silica, and the working wavelength is λ. The values of the coefficients are $B_1 = 0.696263$, $C_1 = 0.0046914826$ μm^2, $B_2 = 0.4079426$, $C_2 = 0.0135120631$ μm^2, $B_3 = 0.8974794$, and $C_3 = 97.9340025$ μm^2 [34]. Additionally, the gold permittivity can be calculated using the Drude–Lorentz model described in ref. [35].

The suggested sensor's probable construction approach is shown in Fig. 1 (b). To create the fiber, all the capillaries and solid rods are stacked together and then drawn at a specified pace, which is known as the stack and drawn technique [31], [36]. To make and eliminate air holes, thick capillary and solid rods are utilized, correspondingly. After the fiber has been fabricated, the polishing technique is applied to create the D-shaped surface where gold is coated [36], [37].

Fig. 1 (c) illustrates a configuration of how the proposed PCF biosensor can be used to detect bacteria in a test sample. Optical Tunable Source (OTS) launches optical light across single-mode fiber (SMF). A splicing technique allows the SMF and the suggested sensor to be merged. There is an analyte in the flow cell that travels across the gold layer in this suggested experimental setup. A pump can be used to regulate the flow of analyte samples in and out of the

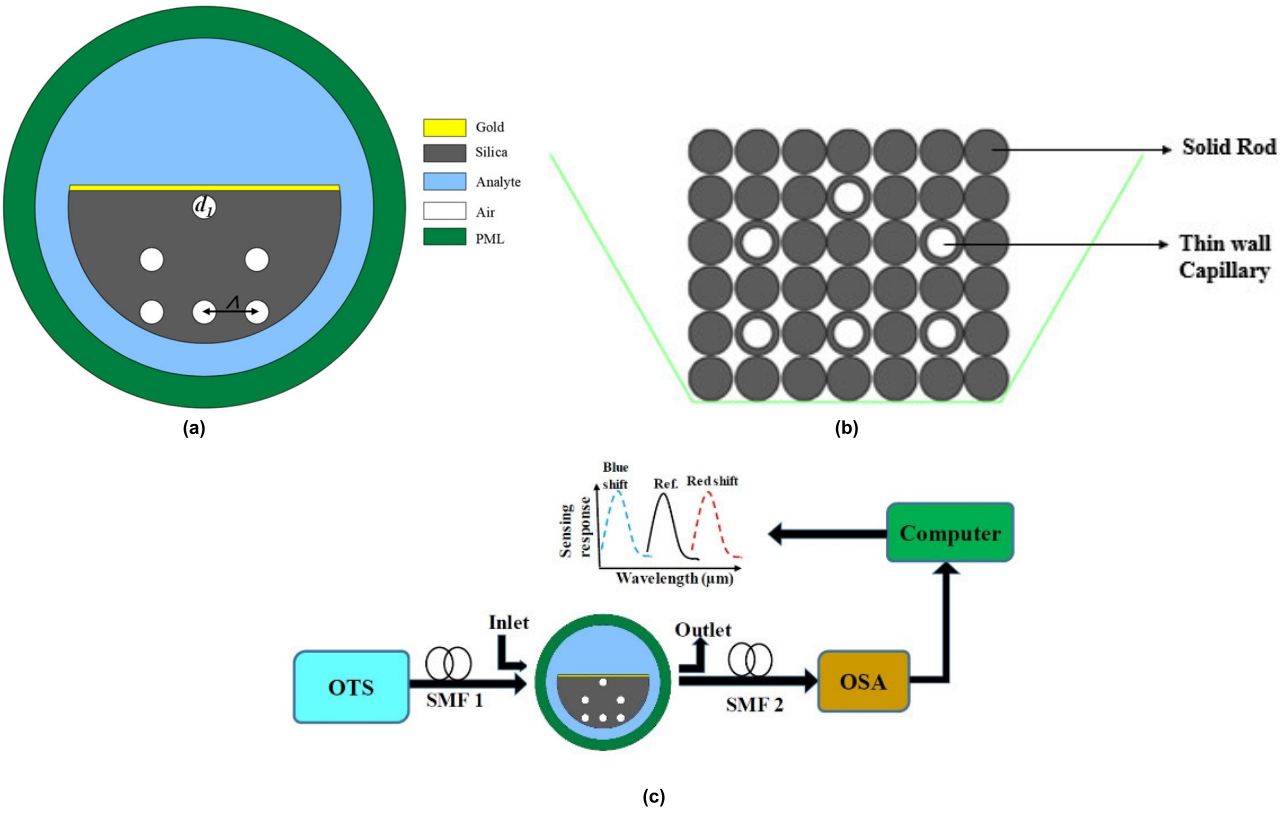

FIGURE 1. (a) Schematic diagram of the proposed PCF biosensor, (b) Fiber's fabrication arrangement, and (c) Suggested experimental setup.

chamber. First, the sensor probes need to be cleaned with de-ionized water. The effective refractive index of the SPP mode is shifted by the interaction of the analyte. As a result, the SMF is used to receive directed light for analysis by the Optical Spectrum Analyzer (OSA). An output spectrum is now visible on the computer screen.

III. WORKING PRINCIPLE, RESULTS, AND DISCUSSION

In this work, the proposed PCF-SPR sensor was simulated and analyzed using the commercial COMSOL Multiphysics electromagnetic simulation software. To absorb the radiation power, a perfectly matched layer (PML) was added to the fiber's outermost layer. When the simulation was conducted, the physics-controlled mesh was regarded excellent and capable of achieving the highest level of simulation precision.

For the proposed PCF biosensor, Core-guided and plasmon-polariton modes of optical field patterns are presented in Fig. 2 (a) and (b). Photonic crystal fibers have air holes that act as their cladding area. When light is transmitted, the entire optical spectrum is confined to the fundamental core guided mode. As an alternative, the mode of plasmonic polariton can only be observed in the presence of material that has already been placed in the detection medium. Incoming light from the core mode and surface plasmonic waves from the SPP mode have equal wave vectors in the resonance state, which is also known as the phase-matching state. When the surface plasmon resonance (SPR) condition is present, as in Fig. 2(c), the field variations can be seen. Because of the phase-matching condition, a substantial amount of energy transfer has been seen because of the plasmonic material covering and the dielectric layer's strong connection. First-order fundamental mode, second order SPP mode, and loss curve of the water sample with *Vibrio Cholera* bacterium are presented in Fig. 2 (d)'s dispersion relationship. The refractive index value of the contaminated water is 1.365, so the indices of refraction of the basic core guided mode and the SPP mode match at 1.56 μm operating wavelength, resulting in a considerable coupling between these two modes and a large peak loss at the intersection location. Excitation of free electrons in the transversal electric mode, which is y-polarized rather than x-polarized, has resulted in a substantial evanescent field in this PCF-SPR structure. Under the phase-matching state, a considerable quantity of energy was transferred from the core mode to the plasmon-polariton mode. The phenomena of optical field distribution and mode coupling of the proposed PCF-SPR biosensor can be understood further by following the coupled-mode theory given in Ref. [38].

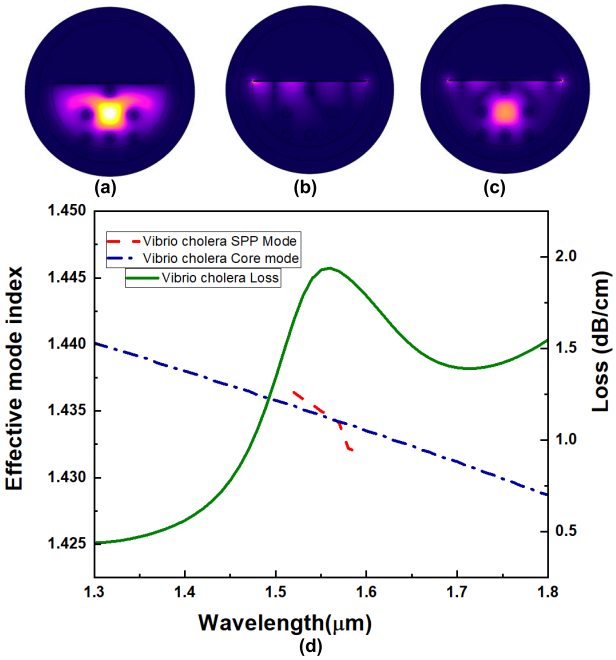

FIGURE 2. Light field distribution of (a) Core mode, (b) SPP mode, (c) SPR mode (d) Dispersion relation of core-guided mode, SPP mode, and their loss spectra.

PCF-based SPR biosensor's performance can be improved by reducing core mode confinement loss and it can be described using the following equation no. 2 [39].

$$\alpha = \frac{40\pi\, Im(n_{eff})}{In(10)\lambda} \approx 8.686 \times k_0 Im(n_{eff}) \times 10^4\ dB/cm \qquad (2)$$

where, $k_0 = 2\pi/\lambda$ is the wave number in free space, λ is the operating wavelength, and Im (n_{eff}) is the imaginary part of the effective index.

The Wavelength sensitivities (WS) can be defined using the following equation no. 3 [39].

$$WS\ [nm/RIU] = \frac{\Delta\lambda_{peak}}{\Delta n_a} \qquad (3)$$

where $\Delta\lambda_{peak}$ is the peak shift, and Δn_a is the variation of analyte RI.

Samples of pure water and contaminated water with various bacteria are inserted into the proposed PCF biosensor, and the resonance wavelength of the loss curve is monitored to identify water contamination due to bacteria. Resonance wavelengths of pure and contaminated water are distinct if the samples are infected with bacteria because the RI of pure and contaminated water differs. Fig. 3 illustrates the confinement losses of pure and contaminated water due to *Vibrio Cholera* (RI: 1.365), *E. Coli* (RI: 1.388), *Bacillus Anthracis* (RI: 1.3833), and *Enterococcus Faecalis* (RI: 1.3921), respectively [18], [40]. The RI of pure water changes to 1.365, 1.388, 1.3833, and 1.3921 for the presence of single bacterium (one molecule) *Vibrio Cholera, E. Coli, Bacillus Anthracis,* and *Enterococcus Faecalis*, respectively [41], [41], [42]. The confinement loss of 0.63369 dB/cm and the resonant wavelength at 1.43 μm for the pure water are observed by the red curve as shown in Fig. 3. On the contrary, the confinement losses of 1.9393 dB/cm, 7.0772 dB/cm, 5.1457 dB/cm, and 9.6294 dB/cm at resonant wavelengths of 1.56 μm, 1.71 μm, 1.67 μm, and 1.74 μm for the contaminated water are noticed by the blue curves as illustrated in Fig. 3. Wavelength sensitivities (WS) of the proposed PCF biosensor have been calculated 3714 nm/ RIU, 4827 nm/RIU, 4502 nm/RIU, and 5161 nm/RIU for identifying *Vibrio Cholera, E. Coli, Bacillus Anthracis,* and *Enterococcus Faecalis* Cell, respectively in the water. WS of the proposed sensor was improved by establishing strong coupling between the core guided mode and surface plasmon polariton mode. This was done by creating a d-shaped structure of the fiber which enabled great matching of wave vectors of the transmitted light and surface plasmonic wave of the proposed PCF-SPR.

The impacts of structural parameters' (Pitch, Au thickness, air hole diameter) variation of the proposed biosensor for the *Vibrio Cholera* bacteria have been observed. In Fig. 4 (a), redshifting is observed when the magnitude of d_1 is changed from 1.40 μm to 1.6 μm and the propagation loss is increased. An increase in the amount of energy that can be transferred from the fundamental mode to the surface plasmon polariton mode is caused by enhancing the coupling strength between the two modes as d_1 increases and vice-versa.

Fig. 4 (b) shows the impact of gold thickness on the loss curves of the water with *Vibrio Cholera* bacteria. When the gold layer is increased from 150 nm to 250 nm, blueshifting is noticed. Changes in both the SPP and core mode refractive indices occur when the proposed PCF-SPR's Au thickness is varied. The phase matching point has been relocated to shorter wavelengths because of this. When the coupling strength between the core mode and the SPP mode is reduced, the propagation loss decreases. Blueshifting with confinement loss being decreased also occurs while tuning the pitch value from 3.2 μm to 3.4 μm for the proposed biosensor as depicted in Fig. 5 (a). With an R-square value of 0.99904, the polynomial fit curve generated an excellent fit, as illustrated in Fig. 5 (b).

As depicted in Figure 6 (a), (b), and (c), air-hole diameter, gold-plasmonic thickness, and the pitch value, respectively all influence wavelength sensitivity for detecting *Enterococcus Faecalis* bacteria in pure water. The diameter of the airhole is 1.5 μm, the thickness of the gold is 200 nm, and the pitch value is 3.3 μm, resulting in highest WS of 5161 nm/RIU for the proposed sensor. As a result, these values were chosen as the most optimized ones for the proposed PCF-SPR sensor.

Certain critical characteristics, such as signal–to–noise ratio (SNR) and detection limit (φn) are proportional to the full width at half maxima ($\Delta\lambda_{1/2}$) of the loss spectra and can

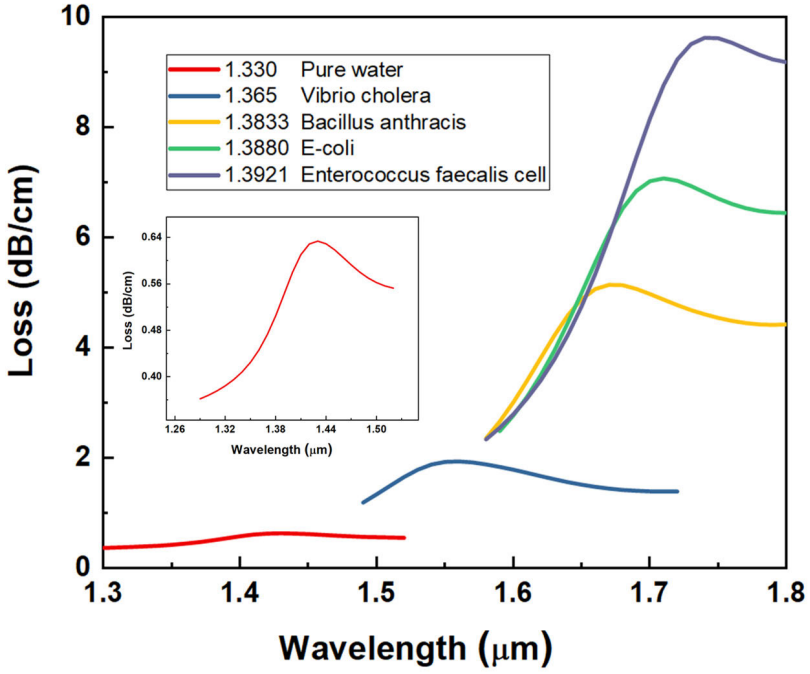

FIGURE 3. Loss curves of pure water, *Vibrio Cholera*, *Bacillus anthracis*, *E. coli*, and *Enterococcus faecalis*.

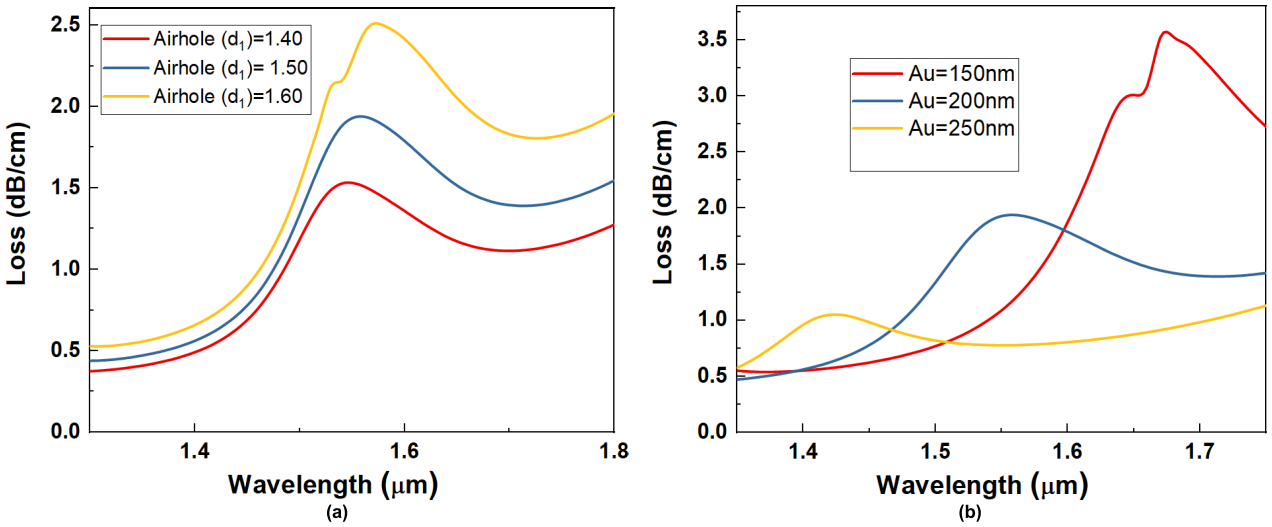

FIGURE 4. Loss curves due to parametric variation (a) d_1 and (b) Au.

be determined using the following equations 4 and 5 [43].

$$SNR = \frac{\Delta\lambda_{peak}}{\Delta\lambda_{1/2}} \tag{4}$$

$$\varphi_n = \frac{\Delta\lambda_{1/2}}{1.5x\ (SNR)^{0.25}} \tag{5}$$

For different bacteria, the suggested sensor's signal-to-noise ratio SNR and detection limit (DL) are shown in Fig. 7.

An improved sensor SNR can be achieved by decreasing the sensor's full width at half maximum (FWHM). In order to determine the sensor's SNR and detection limit (DL), equations 4 and 5 are employed. The highest SNR and DL values were found to be 1.29 and 375.4 for *Vibrio Cholera* and *Enterococcus Faecalis Cell*, respectively.

Equation 6 relates the propagation length or sensor length of a sensor to the confinement loss [43]. Table 1 summarizes the SNR, DL and sensor lengths of the proposed sensor for various bacteria.

$$S_l = \frac{1}{\alpha} \tag{6}$$

The quality factor and the detection accuracy (DA) of the proposed sensor is calculated from equation 7 and 8 which

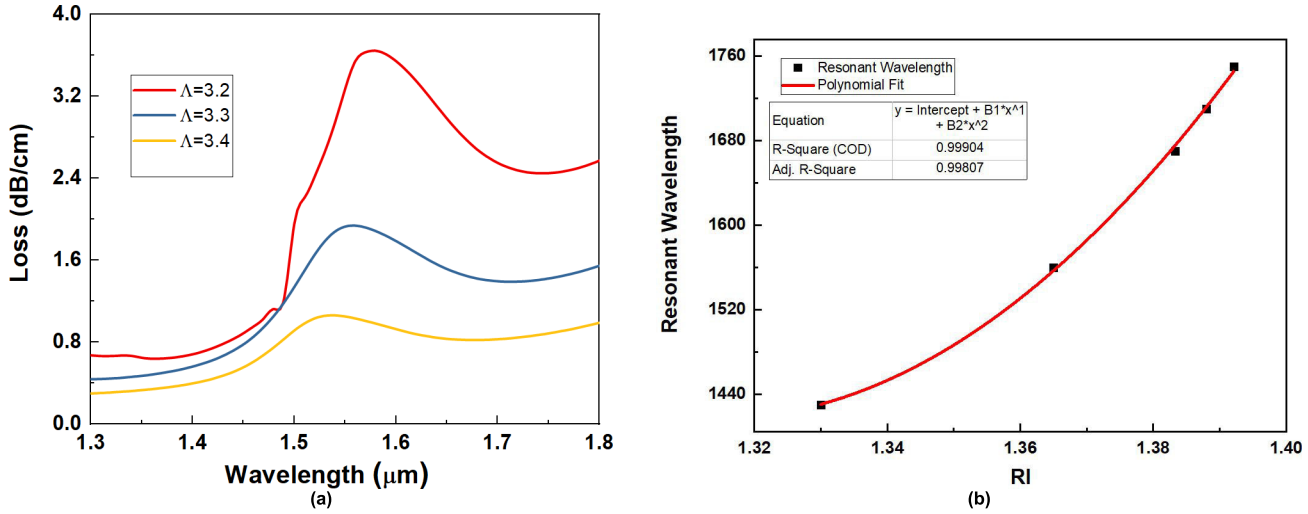

FIGURE 5. Loss curves due to parametric variation (a) Pitch value and (b) Polynomial fit of resonant wavelengths.

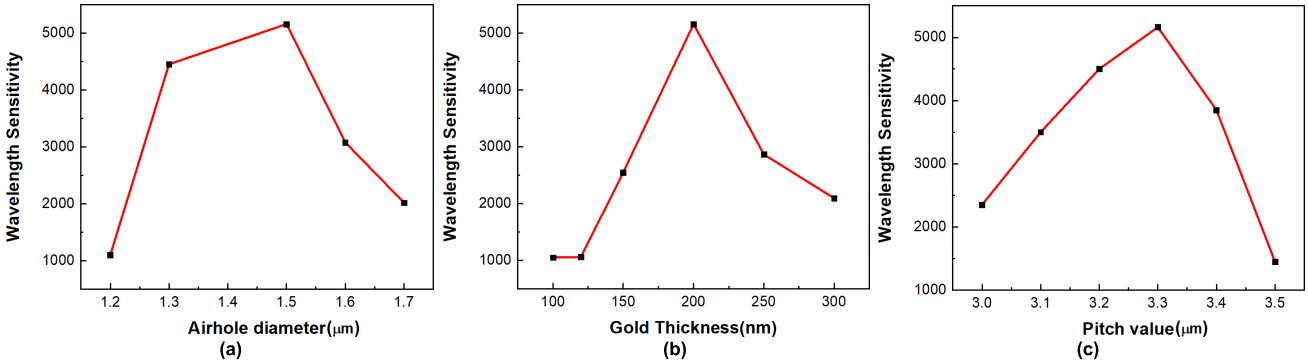

FIGURE 6. Wavelength sensitivity of enterococcus faecalis due to variation of (a) Airhole diameter, (b) Gold thickness, and (c) Pitch value.

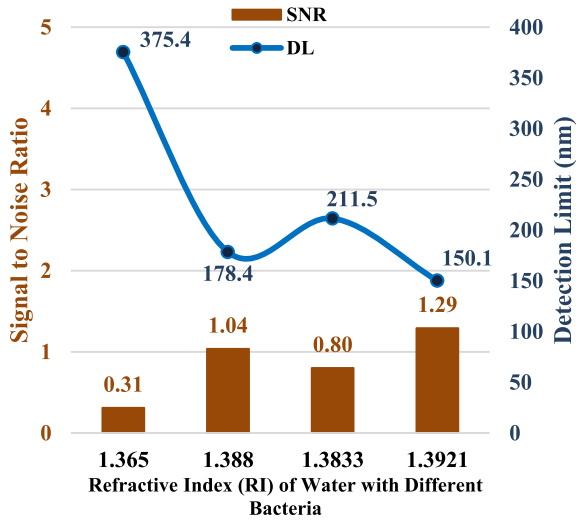

FIGURE 7. SNR and DL of the proposed PCF.

are given following [43]:

$$Q = \frac{WS}{\Delta\lambda_{1/2}} \tag{7}$$

$$DA = \frac{1}{\Delta\lambda_{1/2}} \tag{8}$$

Propagation loss which is a key structural characteristic of a PCF-based sensor, and is critical for the sensor or propagation length, is influenced by the air hole rings in its cladding, as well as their diameter and pitch. To further enhance confinement, it is important to consider factors like core diameter and operating wavelength. Light leakage from the core is minimized by keeping air holes as close together as possible, resulting in less light loss from the cladding area. An important measure that is dependent on confinement loss is the sensor length or propagation length. The proposed PCF biosensor's WS increases while the sensor's length decreases for contaminated water with different bacteria, as shown in Fig. 8 (a). Equation 6 was used to derive sensor lengths (Sl) of the proposed sensor for different bacteria. Quality factor and the detection accuracy of the proposed sensor has been also calculated and illustrated in Fig. 8 (b). Table 1 presents the proposed biosensor's possible significant performance parameters such as SNR, DL, SL, Limit of Detection, Quality Factor, and DA. It has been observed that

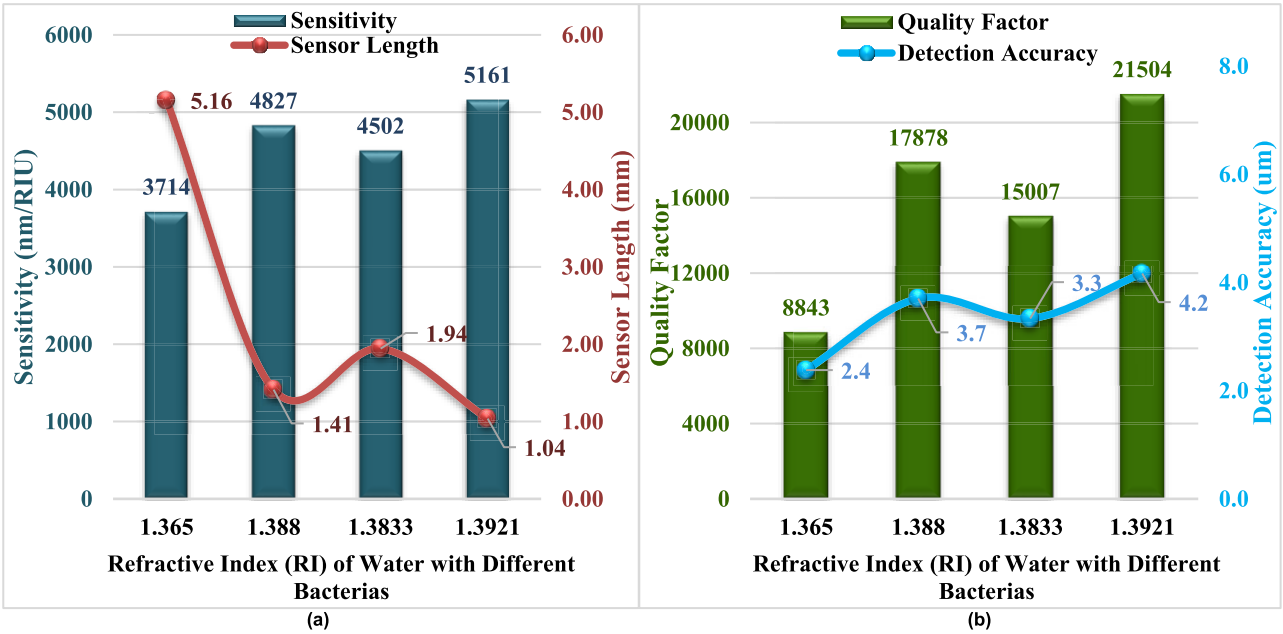

FIGURE 8. (a) Sensitivity and sensor length, (b) Quality factor and detection accuracy.

TABLE 1. Performance parameters comparison of the proposed PCF-SPR biosensor with recently published works.

Bacteria	Method	SNR	DL (nm)	SL (mm)	Limit of Detection	Quality Factor	DA (μm)	Ref.
Pseudomonas Bacteria	Surface Plasmon Resonance	-	-	-	370°/RIU	86.25	-	[44]
E. coli	Surface Plasmon Resonance	-	-	36	1929 nm/RIU	-	-	[45]
Vibrio Cholera	Surface Plasmon Resonance	0.31	375.4	5.16	3714 nm/RIU	8843	2.4	This Work
E. coli	Surface Plasmon Resonance	1.04	178.4	1.41	4827 nm/RIU	17878	3.7	This Work
Bacillus Anthracis	Surface Plasmon Resonance	0.80	211.5	1.94	4502 nm/RIU	15007	3.3	This Work
Enterococcus Faecalis	Surface Plasmon Resonance	1.29	150.1	1.04	5161 nm/RIU	21504	4.2	This Work

the proposed biosensor achieved excellent performance characteristics compared to the other reported biosensors. Greater Quality Factor has been achieved by the proposed biosensor than the work reported in Ref. [44]. The proposed sensor's length is also calculated as very small compared to the sensor reported in Ref [45]. Maximum WS of 5161 nm/RIU and minimum WS of 3714 nm/RIU have been obtained by the proposed PCF-SPR biosensor to detect *Enterococcus Faecalis* and *Vibrio Cholera* bacteria in drinking water, respectively.

IV. CONCLUSION

A simple square lattice, single layer air hole configured PCF biosensor was proposed which can detect pathogenic bacteria in drinking water. Gold was chosen as the plasmonic material and coated over the d-shaped surface of the proposed biosensor. The proposed biosensor achieved WS of 3714 nm/RIU, 4827 nm/RIU, 4502 nm/RIU, and 5161 for *Vibrio cholera, E. coli, Bacillus anthracis, and Enterococcus faecalis* bacteria respectively. The proposed biosensor also obtained the highest SNR and DL values of 1.29 and 375.4 for *Vibrio Cholera* and *Enterococcus Faecalis* bacteria, respectively. While detecting *Enterococcus Faecalis* bacteria, the proposed sensor achieved highest quality factor and detection accuracy of 21504 and 4.2 μm, respectively. The structural complexity of the proposed sensor is minimum, and it is feasible for fabrication. Hence, the proposed sensor can be a suitable candidate for the real-time application of bacteria detection from drinking water.

REFERENCES

[1] D. N. Magana-Arachchi and R. P. Wanigatunge, "Ubiquitous waterborne pathogens," in *Waterborne Pathogens*. PubMed Central, Feb. 2020, pp. 15–42. [Online]. Available: https://www.ncbi.nlm.nih.gov/pmc/articles/PMC7173459/ and https://www.sciencedirect.com/science/article/pii/B9780128187838000025?via%3Dihub

[2] P. Y. Liu, L. K. Chin, W. Ser, T. C. Ayi, P. H. Yap, T. Bourouina, and Y. Leprince-Wang, "An optofluidic imaging system to measure the biophysical signature of single waterborne bacteria," *Lab Chip*, vol. 14, no. 21, pp. 4237–4243, 2014.
[3] J. Kang and M.-G. Kim, "Advancements in DNA-assisted immunosensors," *BioChip J.*, vol. 14, no. 1, pp. 18–31, Mar. 2020.
[4] J. Verma, S. Saxena, and S. G. Babu, "ELISA-based identification and detection of microbes," in *Analyzing Microbes: Manual of Molecular Biology Techniques*, D. K. Arora, S. Das, and M. Sukumar, Eds. Berlin, Germany: Springer, 2013, pp. 169–186.
[5] N. Cui, S. Su, P. Sun, Y. Zhang, N. Han, and Z. Cui, "Isolation and pathogenic analysis of virulent Marek's disease virus field strain in China," *Poultry Sci.*, vol. 95, no. 7, pp. 1521–1528, Jul. 2016.
[6] A. Eparvier and C. Alabouvette, "Use of ELISA and GUS-transformed strains to study competition between pathogenic and non-pathogenic *Fusarium oxysporum* for root colonization," *Biocontrol Sci. Technol.*, vol. 4, no. 1, pp. 35–47, 1994.
[7] Y.-P. Ho and P. M. Reddy, "Identification of pathogens by mass spectrometry," *Clin. Chem.*, vol. 56, no. 4, pp. 525–536, Apr. 2010.
[8] I. O. K'Owino and O. A. Sadik, "Impedance spectroscopy: A powerful tool for rapid biomolecular screening and cell culture monitoring," *Electroanalysis*, vol. 17, no. 23, pp. 2101–2113, Dec. 2005.
[9] Y. Li, Y. T. H. Cu, and D. Luo, "Multiplexed detection of pathogen DNA with DNA-based fluorescence nanobarcodes," *Nature Biotechnol.*, vol. 23, no. 7, pp. 885–889, Jul. 2005.
[10] F. Louws, J. Rademaker, and F. de Bruijn, "The three DS of PCR-based genomic analysis of phytobacteria: Diversity, detection, and disease diagnosis," *Annu. Rev. Phytopathol.*, vol. 37, no. 1, pp. 81–125, 1999.
[11] J. Patel, "16S rRNA gene sequencing for bacterial pathogen identification in the clinical laboratory," *Mol. Diagnosis*, vol. 6, no. 4, pp. 313–321, Dec. 2001.
[12] C. Pruzzo, C. A. GuzmÃİn, and B. Dainelli, "Incidence of hemagglutination activity among pathogenic and non-pathogenic *Bacteroides fragilis* strains and role of capsule and pili in HA and adherence," *FEMS Microbiol. Lett.*, vol. 59, nos. 1–2, pp. 113–118, May 1989.
[13] J.-H. Park, Y.-W. Cho, and T.-H. Kim, "Recent advances in surface plasmon resonance sensors for sensitive optical detection of pathogens," *Biosensors*, vol. 12, no. 3, p. 180, Mar. 2022.
[14] P. Singh, T. Onodera, Y. Mizuta, K. Matsumoto, N. Miura, and K. Toko, "Dendrimer modified biochip for detection of 2,4,6 trinitrotoluene on SPR immunosensor: Fabrication and advantages," *Sens. Actuators B, Chem.*, vol. 137, no. 2, pp. 403–409, Apr. 2009.
[15] A. G. Brolo, "Plasmonics for future biosensors," *Nature Photon.*, vol. 6, no. 11, pp. 709–713, Nov. 2012.
[16] A. M. Shrivastav, U. Cvelbar, and I. Abdulhalim, "A comprehensive review on plasmonic-based biosensors used in viral diagnostics," *Commun. Biol.*, vol. 4, no. 1, Dec. 2021.
[17] J. Homola and M. Piliarik, "Surface plasmon resonance (SPR) sensors," in *Surface Plasmon Resonance Based Sensors*. Berlin, Germany: Springer, 2006, pp. 45–67.
[18] V. Sharma and V. L. Kalyani, "Designing four channel nano cavities coupled photonic crystal based bio-sensor for detection in water bactria," in *Proc. Int. Conf. Comput. Commun. Technol. Smart Nation (IC3TSN)*, Oct. 2017, pp. 84–88.
[19] H.-T. Huang, C.-Y. Huang, T.-R. Ger, and Z.-H. Wei, "Anti-integrin and integrin detection using the heat dissipation of surface plasmon resonance," *Appl. Phys. Lett.*, vol. 102, no. 11, Mar. 2013, Art. no. 111109.
[20] J. Kim, S. H. Chun, L. Amornkitbamrung, C. Song, J. S. Yuk, S. Y. Ahn, B. W. Kim, Y. T. Lim, B.-K. Oh, and S. H. Um, "Gold nanoparticle clusters for the investigation of therapeutic efficiency against prostate cancer under near-infrared irradiation," *Nano Converg.*, vol. 7, no. 1, Dec. 2020.
[21] D. P. Kalogianni, "Nanotechnology in emerging liquid biopsy applications," *Nano Converg.*, vol. 8, no. 1, Dec. 2021.
[22] Y. Chen, B. Ai, and Z. J. Wong, "Soft optical metamaterials," *Nano Converg.*, vol. 7, no. 1, Dec. 2020.
[23] M. F. Prodanov, N. V. Pogorelova, A. P. Kryshtal, A. S. Klymchenko, Y. Mely, V. P. Semynozhenko, A. I. Krivoshey, Y. A. Reznikov, S. N. Yarmolenko, J. W. Goodby, and V. V. Vashchenko, "Thermodynamically stable dispersions of quantum dots in a nematic liquid crystal," *Langmuir*, vol. 29, no. 30, pp. 9301–9309, Jul. 2013.
[24] S. Wadhwa, A. T. John, S. Nagabooshanam, A. Mathur, and J. Narang, "Graphene quantum dot-gold hybrid nanoparticles integrated aptasensor for ultra-sensitive detection of vitamin D3 towards point-of-care application," *Appl. Surf. Sci.*, vol. 521, Aug. 2020, Art. no. 146427.
[25] A. B. Dahlin, "Sensing applications based on plasmonic nanopores: The hole story," *Analyst*, vol. 140, no. 14, pp. 4748–4759, 2015.
[26] B. D. Gupta and R. K. Verma, "Surface plasmon resonance-based fiber optic sensors: Principle, probe designs, and some applications," *J. Sensors*, vol. 2009, Aug. 2009, Art. no. 979761.
[27] M. Shinn and W. M. Robertson, "Surface plasmon-like sensor based on surface electromagnetic waves in a photonic band-gap material," *Sens. Actuators B, Chem.*, vol. 105, no. 2, pp. 360–364, Mar. 2005.
[28] A. A. Rifat, G. A. Mahdiraji, Y. M. Sua, Y. G. Shee, R. Ahmed, D. M. Chow, and F. R. M. Adikan, "Surface plasmon resonance photonic crystal fiber biosensor: A practical sensing approach," *IEEE Photon. Technol. Lett.*, vol. 27, no. 15, pp. 1628–1631, Aug. 1, 2015.
[29] A. Rifat, G. Mahdiraji, D. Chow, Y. Shee, R. Ahmed, and F. Adikan, "Photonic crystal fiber-based surface plasmon resonance sensor with selective analyte channels and graphene-silver deposited core," *Sensors*, vol. 15, no. 5, pp. 11499–11510, May 2015.
[30] F. Haider, R. A. Aoni, R. Ahmed, M. S. Islam, and A. E. Miroshnichenko, "Propagation controlled photonic crystal fiber-based plasmonic sensor via scaled-down approach," *IEEE Sensors J.*, vol. 19, no. 3, pp. 962–969, Feb. 2019.
[31] D. Pysz, I. Kujawa, R. Stepien, M. Klimczak, A. Filipkowski, M. Franczyk, L. Kociszewski, J. Buzniak, K. Harasny, and R. Buczynski, "Stack and draw fabrication of soft glass microstructured fiber optics," *Bull. Polish Acad. Sci., Tech. Sci.*, vol. 62, no. no. 4, pp. 667–682, 2014.
[32] A. Jilani, M. S. Abdel-wahab, and A. HosnyHammad, "Advance deposition techniques for thin film and coating," in *Modern Technologies for Creating the Thin-film Systems and Coatings*. London, U.K.: IntechOpen, 2017. [Online]. Available: https://www.intechopen.com/chapters/52684, doi: 10.5772/65702.
[33] K. Nielsen, D. Noordegraaf, T. Sørensen, A. Bjarklev, and T. P. Hansen, "Selective filling of photonic crystal fibres," *J. Opt., Pure Appl. Opt.*, vol. 7, no. 8, pp. L13–L20, Jul. 2005.
[34] N. Ayyanar, G. T. Raja, M. Sharma, and D. S. Kumar, "Photonic crystal fiber-based refractive index sensor for early detection of cancer," *IEEE Sensors J.*, vol. 18, no. 17, pp. 7093–7099, Sep. 2018.
[35] G. P. Mishra, D. Kumar, V. S. Chaudhary, and G. Murmu, "Cancer cell detection by a heart-shaped dual-core photonic crystal fiber sensor," *Appl. Opt.*, vol. 59, no. 33, pp. 10321–10329, Nov. 2020.
[36] D. K. Sharma, A. Sharma, and S. M. Tripathi, "Characteristics of solid-core square-lattice microstructured optical fibers using an analytical field model," *Opt. Laser Technol.*, vol. 96, pp. 97–106, Nov. 2017.
[37] A. A. Noman, E. Haque, M. A. Hossain, N. H. Hai, Y. Namihira, and F. Ahmed, "Sensitivity enhancement of modified D-shaped microchannel PCF-based surface plasmon resonance sensor," *Sensors*, vol. 20, no. 21, p. 6049, Oct. 2020.
[38] Z. Zhang, Y. Shi, B. Bian, and J. Lu, "Dependence of leaky mode coupling on loss in photonic crystal fiber with hybrid cladding," *Opt. Exp.*, vol. 16, no. 3, pp. 1915–1922, Jan. 2008.
[39] E. Haque, A. A. Noman, M. A. Hossain, N. Hoang Hai, Y. Namihira, and F. Ahmed, "Highly sensitive D-shaped plasmonic refractive index sensor for a broad range of refractive index detection," *IEEE Photon. J.*, vol. 13, no. 1, Feb. 2021, Art. no. 4800211, doi: 10.1109/JPHOT.2021.3055234.
[40] S. Kulkarni, N. Khan, P. Sharan, and B. Ranjith, "Bacterial analysis of drinking water using photonic crystal based optical sensor," in *Proc. 7th Int. Conf. Comput. Sustain. Global Develop. (INDIACom)*, Mar. 2020, pp. 186–191.
[41] H. J. Coles, B. R. Jennings, and V. J. Morris, "Refractive index increment measurement for bacterial suspensions," *Phys. Med. Biol.*, vol. 20, no. 2, p. 310, 1975.
[42] H. Sarker, F. Alam, M. R. Khan, M. A. Mollah, M. L. Hasan, and A. B. M. S. Rafi, "Designing highly sensitive exposed core surface plasmon resonance biosensors," *Opt. Mater. Exp.*, vol. 12, no. 5, p. 1977, 2022.
[43] P. Y. Liu, L. K. Chin, W. Ser, T. C. Ayi, P. H. Yap, T. Bourouina, and Y. Leprince-Wang, "Real-time measurement of single bacterium's refractive index using optofluidic immersion refractometry," *Proc. Eng.*, vol. 87, pp. 356–359, Jan. 2014.

[44] Y. Vasimalla, H. S. Pradhan, and R. J. Pandya, "Sensitivity enhancement of the SPR biosensor for pseudomonas bacterial detection employing a silicon-barium titanate structure," *Appl. Opt.*, vol. 60, no. 19, p. 5588, 2021.

[45] K. Dandapat, S. M. Tripathi, Y. Chinifooroshan, W. J. Bock, and P. Mikulic, "Compact and cost-effective temperature-insensitive bio-sensor based on long-period fiber gratings for accurate detection of E coli bacteria in water," *Opt. Lett.*, vol. 41, no. 18, p. 4198, 2016.

EMRANUL HAQUE received the B.Sc. and M.Sc. degrees in electrical and electronic engineering from Independent University, Bangladesh (IUB), in 2014 and 2018, respectively. He is currently a Lecturer with the Department of Electrical and Electrical Engineering, IUB. His research interests include optical sensors, plasmonics, biosensors, and wearable antennas.

ABDULLAH AL NOMAN (Member, IEEE) received the B.Sc. and M.Sc. degrees in electrical and electronic engineering from Independent University, Bangladesh, Dhaka, Bangladesh, in 2018 and 2019, respectively. He is currently employed as a Research Associate and an Adjunct Lecturer with the Department of Electrical and Electronic Engineering, Independent University, Bangladesh. His research interests include optical biosensors, plasmonics, photonic crystal fiber, patch antennas, and embedded systems.

FEROZ AHMED (Member, IEEE) received the B.Sc. degree in electrical and electronic engineering from the Rajshahi University of Engineering and Technology, Bangladesh, in 1995, the M.Sc. degree in electrical engineering from the Universiti Teknologi Malaysia, Malaysia, in 1998, and the Ph.D. degree in optical fiber communication from The University of Electro-Communications, Tokyo, Japan, in 2002. From 2002 to 2005, he was a Postdoctoral Research Fellow with Gunma University, Gunma, and The University of Electro-Communications. In 2005, he was appointed as an Assistant Professor with the School of Engineering and Computer Science, Independent University, Bangladesh, and became an Associate Professor and a Professor, in 2011 and 2020, respectively. He has published over 90 papers in different peer-reviewed international journals and conferences. His current research interests include photonics and microwave sensors, fiber-optics, antenna, wireless communication systems, and non-invasive biomedical sensing systems.